HHS Public Access

Author manuscript

Clin Cancer Res. Author manuscript; available in PMC 2015 March 24.

Published in final edited form as:

Clin Cancer Res. 2009 March 15; 15(6): 1989–1997. doi:10.1158/1078-0432.CCR-08-2054.

Pathologic Correlates of Primary Central Nervous System Lymphoma Defined in an Orthotopic Xenograft Model

Cigall Kadoch[1], **Eduard B. Dinca**[2], **Ramona Voicu**[2], **Lingjing Chen**[1], **Diana Nguyen**[1], **Seema Parikh**[3], **Juliana Karrim**[1], **Marc A. Shuman**[1,5], **Clifford A. Lowell**[4], **Patrick A. Treseler**[3,5], **C. David James**[2,5], and **James L. Rubenstein**[1,5]

[1]Division of Hematology/Oncology, University of California at San Francisco, San Francisco, California

[2]Department of Neurological Surgery, University of California at San Francisco, San Francisco, California

[3]Department of Pathology, University of California at San Francisco, San Francisco, California

[4]Department of Laboratory Medicine, University of California at San Francisco, San Francisco, California

[5]Helen Diller Comprehensive Cancer Center, University of California at San Francisco, San Francisco, California

Abstract

Purpose—The prospect for advances in the treatment of patients with primary central nervous system lymphoma (PCNSL) is likely dependent on the systematic evaluation of its pathobiology. Animal models of PCNSL are needed to facilitate the analysis of its molecular pathogenesis and for the efficient evaluation of novel therapeutics.

Experimental Design—We characterized the molecular pathology of CNS lymphoma tumors generated by the intracerebral implantation of Raji B lymphoma cells in athymic mice. Lymphoma cells were modified for bioluminescence imaging to facilitate monitoring of tumor growth and response to therapy. In parallel, we identified molecular features of lymphoma xenograft histopathology that are evident in human PCNSL specimens.

Results—Intracerebral Raji tumors were determined to faithfully reflect the molecular pathogenesis of PCNSL, including the predominant immunophenotypic state of differentiation of lymphoma cells and their reactive microenvironment. We show the expression of interleukin-4 by Raji and other B lymphoma cell lines *in vitro* and by Raji tumors *in vivo* and provide evidence for

Requests for reprints: James L. Rubenstein, Division of Hematology/Oncology, University of California at San Francisco, 505 Parnassus Avenue, Suite M1282, Box 1270, San Francisco, CA 94143-1270. Phone: 415-502-4430; Fax: 415-476-4943; jamesr@medicine.ucsf.edu.

A portion of this work was presented in abstract form at the 2008 AACR Annual Meeting.

Disclosure of Potential Conflicts of Interest

No potential conflicts of interest were disclosed.

a role of this cytokine in the M2 polarization of lymphoma macrophages both in the murine model and in diagnostic specimens of human PCNSL.

Conclusion—Intracerebral implantation of Raji cells results in a reproducible and invasive xenograft model, which recapitulates the histopathology and molecular features of PCNSL, and is suitable for preclinical testing of novel agents. We also show for the first time the feasibility and accuracy of tumor bioluminescence in the monitoring of a highly infiltrative brain tumor.

Primary central nervous system lymphoma (PCNSL) is defined as a high-grade lymphoma presenting in the brain or spinal cord in the absence of systemic lymphoma. Although the predominant histology of PCNSL is large B-cell lymphoma, Burkitt's, Burkitt-like, lymphoblastic, and T-cell lymphomas may also manifest and be confined to the brain in a manner consistent with PCNSL (1,2).

There is significantly less information regarding the molecular pathogenesis of PCNSL in comparison with systemic non-Hodgkin's lymphoma. Generally, PCNSL appears to be derived from mature B cells, which have been exposed to antigen and have undergone T-cell-dependent affinity maturation in a germinal center microenvironment (3). In support of this conclusion is the fact that the majority of non-AIDS PCNSL tumors express Bcl-6, a germinal center marker. Other characterizations of the immunophenotype of PCNSL have revealed that these tumors exhibit overlapping features of germinal center and activated B-cell differentiation: immunohistochemical analysis shows that the majority of brain lymphomas express MUM-1, a marker of activated B cells, and Bcl-6, a marker of germinal centers (4,5). This latter conclusion is additionally supported by the results of microarray analyses of PCNSL gene expression (6,7). This immunophenotypic stage of differentiation provides a logical basis to explain how a variant of large B-cell lymphoma that usually exhibits germinal center features, including Bcl-6 expression, is generally associated with an inferior outcome relative to systemic lymphomas of the same histology and stage (8,9).

In addition to Bcl-6 and MUM-1, gene expression analyses have revealed ectopic expression of interleukin-4 (IL-4),a B-cell growth factor, by tumor cells and endothelia in PCNSL specimens (7). Moreover, the activation of STAT6, a transcriptional mediator of IL-4-dependent gene expression, was also shown to be expressed by PCNSL cells and tumor endothelia, providing evidence for active IL-4 signaling in CNS lymphoma. Elevated expression of activated STAT6 by lymphoma cells was associated with adverse prognosis in patients treated with high-dose -based chemotherapy, supporting a significant role for IL-4 signal transduction in CNS lymphoma pathogenesis (7).

To date, no animal model of PCNSL has been developed, which recapitulates both histopathologic and molecular features of this disease, including the relevant immunophenotypic state of differentiation of tumor cells and the reactive microenvironment. Given the poor prognosis of PCNSL as well as the severe toxicities associated with established genotoxic therapies, there is a significant need for such models to be applied in the systematic evaluation of novel agents for treating this cancer.

The development of bioluminescence imaging (BLI) has facilitated the noninvasive evaluation of tumor growth and therapeutic response in a variety of cancer xenograft

models, including for brain tumors (10,11). However, this technology has not been applied previously to the study of lymphomatous growth and dissemination in the brain. Here, we report the first intracerebral model of CNS lymphoma, which recapitulates specific aspects of the molecular pathogenesis of this disease and which has been adapted for BLI to serially monitor tumor growth and response to therapy.

Materials and Methods

Tissue culture

Raji, Ramos,2F–7, and EBV-transformed peripheral blood lymphocytes cells were obtained from the American Type Culture Collection. These were cultured at 37°C and 5% CO_2 in high-glucose DMEM-21 supplemented with 1% penicillin-streptomycin,10% FCS, and 1% nonessential amino acids. Raji cells were modified to stably express firefly luciferase (Raji-fl) by lentiviral transduction as described (11).

Surgery

Athymic mice (*nu/nu*; 4–6 weeks old; Simmonsen) were injected in the right cerebral hemisphere with 5×10^5 Raji-fl cells at coordinates 0.5 mm anterior and 2.5 mm lateral from the bregma and at an intraparenchymal depth of 3 mm. Cultured cells were washed three times with PBS, counted, and maintained on ice in DMEM until injection. Mice were anesthetized (ketamine/xylazine) and placed in a stereotactic frame (Stoelting Just-for-Mice) and a Hamilton syringe with 26-gauge needle was used for injection at a volume of 5 μL and at a rate of 1 μL/min, with the needle left in place for 5 min after injection. All animal experiments were done following institutional guidelines.

BLI was conducted using a Xenogen Lumina optical imaging system (Caliper). Mice were anesthetized before intraperitoneal injections of luciferin (D-Luciferin potassium salt; Gold Biotechnology) at a dose of 150 mg/kg, providing a saturating substrate concentration for luciferase enzyme. Peak luminescent signals were consistently recorded 12 min after luciferin injection. Regions of interest encompassing the intracranial area of signal were defined using Living Image software, and the total photons/s/steradian/cm^2 were recorded.

In vivo assessment of temozolomide response

Mice with intracranial Raji-fl cells were imaged 4 days after injection and distributed into two groups (10 each) with equivalent average BLI signal. The temozolomide treatment group received five daily doses of 50 mg/kg by oral gavage for a total dose of 250 mg/kg temozolomide between days 4 and 8 after tumor engraftment. The control group received similar volumes of Ora-Plus, the methylcellulose vehicle used for temozolomide solubilization. Kaplan-Meier survival curves were generated using Prism3 software and the statistical difference between curves was derived with a log-rank test.

Immunohistochemistry, immunofluorescence, and *in situ* hybridization

For immunohistochemical studies, frozen or paraffin sections (8 μm thick) were fixed, blocked, and immunostained with the appropriate antibody: α-CD20 (BD Biosciences), α-Bcl-6 (CellMarque), α-MUM-1 (DAKO), monoclonal α-IL-4 (Santa Cruz Biotechnology),

rabbit polyclonal α-VWF (Santa Cruz Biotechnology), α-pSTAT6 (Upstate), α-CD11b (BD Biosciences), α-CD68 (clone KP1; DAKO), and monoclonal α-factor XIIIa (Biogenex). Affinity-purified polyclonal rabbit α-Ym1 antibody was a kind gift of Dr. Richard Locksley. Immunoreactivity was visualized using the biotin-streptavidin peroxidase method. Immunofluorescence microscopy was done with frozen sections (6–8 μm) that were fixed in 2% formaldehyde, blocked, and subjected to antibody staining with α-IL-4, α-VWF, α-CD68, or α-factor XIIIa. Secondary antibodies conjugated to Alexa Fluor 488 and 594 (Molecular Probes) were used for detection with an Olympus AX70 upright microscope. 4′, 6-Diamidino-2-phenylindole counterstain was used to visualize cell nuclei. Brightness and contrast of images were modified for publication.

For *in situ* hybridization, full-length human IL-4 cDNA in pDNR-Dual (6971781; American Type Culture Collection) was subcloned into pBluescriptSK(-). *In vitro* transcription was done using T3 and T7 polymerase to generate digoxigenin-labeled riboprobes. All tissues used for *in situ* hybridization were snap-frozen in OCT, sliced into frozen sections (16 μm),and stored at −80°C. Sections were then fixed in 4% paraformaldehyde and subjected to proteinase K digestion followed by incubation in 1% Triton X-100. Hybridization was done at 60°C with 400 ng/mL digoxigenin-labeled antisense and sense riboprobes to human IL-4 and the bound probe was detected using alkaline phosphatase-labeled anti-digoxigenin F(ab) (1:5,000 dilution) and NBT/BCIP tablets (Roche Applied Science).

RNA isolation and quantitative reverse transcription-PCR

Lymphoma cell nuclei accounted for at least 70% of all cells in each tumor specimen used in this analysis as determined by histopathologic analysis of H&E-stained sections used in parallel. Tissue sections (14 μm thick) were prepared using a cryostat. For gene expression analysis, these were placed in RLT buffer plus 1% β-mercaptoethanol and homogenized, and RNA was prepared (Qiagen). RNA was quantified based on absorbance at 260 nm, and quality was assured by measuring absorbance 260:280 ratios. Quantitative reverse transcription-PCR (RT-PCR) for determination of human IL-4 and mouse Ym1 (Chi3-L3) RNA expression was done using probe primer sets (Applied Biosystems).

Results

Development of an intracerebral model of invasive CNS lymphoma enabled for BLI

Raji cells were selected for intracranial injection based on their tumorigenicity in mouse models of systemic non-Hodgkin's lymphoma and because of their high relative expression of oncogenes, such as Pim kinases, which are associated with poor prognosis in systemic lymphoma and refractory disease in CNS lymphoma (7,12–14). The Raji cells were modified to stably express firefly luciferase by means of lentiviral transduction as described (11). Modified cells implanted in the brain (5×10^5 per mouse) were found to be highly tumorigenic and exhibited an invasive phenotype with molecular characteristics of PCNSL: $CD20^+$/$Bcl\text{-}6^+$/$MUM\text{-}1^+$,the predominant immunophenotype of PCNSL (refs. 4,5; Fig. 1).

Raji lymphoma cells implanted in the brain are extremely infiltrative, with evidence for leptomeningeal invasion and dissemination into the contralateral hemisphere in nearly every

xenograft, replicating this quintessential feature of PCNSL (Fig. 1). Immunohistochemistry and quantitative RT-PCR showed that Raji cells express cathepsin D, a protease shown previously to be up-regulated in PCNSL pathologic specimens compared with nodal non-Hodgkin's lymphoma specimens and a candidate mediator of CNS lymphoma invasiveness (7). We also used immunohistochemistry and quantitative RT-PCR to show lymphoma xenograft expression of Pim-2 kinase, a prosurvival gene associated with refractory CNS lymphoma and which has also been linked to prostate cancer invasiveness (refs. 13, 15, 16; data not shown).

IL-4 expression in PCNSL

We previously showed significant expression of IL-4 within PCNSL tumors by quantitative RT-PCR and noted a trend between high intratumoral expression of IL-4 and shorter overall survival. We have also applied *in situ* hybridization to investigate intratumoral IL-4 expression within PCNSL diagnostic specimens, the results of which showed that IL-4 RNA was reproducibly expressed by lymphoma cells in PCNSL (7) as well as in cases of nodal large B-cell lymphoma.[6] We therefore evaluated the expression of IL-4 by Raji lymphoma cells *in vitro* using quantitative RT-PCR and determined constitutive IL-4 expression in Raji cells under tissue culture conditions. Similar results were detected in other B lymphoma cell lines analyzed for IL-4 expression including Ramos cells (Fig. 2A) and 2F-7 and EBV-transformed human B-lymphocytes (data not shown). Using species-specific primers for human IL-4, we used quantitative RT-PCR to show that IL-4 expression is induced by >3-fold in Raji cells on intracerebral implantation ($P < 0.03$),suggesting that this multifunctional cytokine participates in CNS lymphomagenesis.

Relative IL-4 RNA levels in Raji intracerebral xenografts were similar to levels in PCNSL tumors, particularly in cases with short survival in which normalized IL-4 RNA expression was between 0.03 and 0.332 (relative to hGUS),supporting the physiologic relevance of these measurements. To our knowledge, this is the first direct demonstration of IL-4 expression by malignant B lymphoma cells *in vitro* or *in vivo*.

We confirmed the intratumoral expression of IL-4 by Raji lymphoma cells in xenografts both by *in situ* hybridization and by immunohistochemical detection methods (Fig. 2B). IL-4 protein was detected predominantly on tumor cells, tumor vasculature, and occasionally tumor-associated macrophages but not within areas of normal brain devoid of tumor infiltration.

Further evidence for IL-4-mediated autocrine as well as paracrine signaling within the Raji xenograft-based CNS lymphoma model was indicated by the expression of activated STAT6 by tumor cell and tumor vasculature, consistent with our demonstration of the expression of IL-4 (and activated STAT6) selectively by tumor vessels in human PCNSL tumors (ref. 7; Fig. 3A). By contrast, tumor angiogenesis in response to intracerebral implantation of human glioblastoma cells was not associated with expression of IL-4 or activated STAT6 (Fig. 3B).

[6]Unpublished observations.

M2 macrophage polarization in PCNSL

A recent analysis of the cerebrospinal fluid proteome in brain tumor patients showed that tryptic peptides derived from CD14, a marker of activated macrophages, are significantly up-regulated in patients with CNS lymphoma (17). Based on this observation, which suggests that macrophage activation may be a prominent feature of the disease, as well as the evidence for a significant pathologic role of tumor-associated macrophages in cancer (18–22),we pursued the characterization of the phenotypic differentiation of intratumoral macrophages within our model. We determined that the intracerebral implantation of Raji cells results in profound intratumoral infiltration of macrophages, often concentrated around blood vessels, as shown by staining for CD11b (Mac-1),a monocyte/macrophage marker (Fig. 4A and B). There was minimal or absent CD11b immunoreactivity in areas of normal brain.

Given our demonstration of the endogenous expression of IL-4 by tumor cells and by other cells within the microenvironment in human PCNSL, we hypothesized that a significant proportion of intratumoral macrophages in the xenograft model would express Ym1 (chitinase-3-like 3),one of the most highly induced IL-4 target genes and an established marker of IL-4-induced M2 polarization of murine macrophages (23,24). Immunohistochemical analysis revealed significant expression of Ym1 by the majority of tumor-associated macrophages in Raji intracranial xenografts as evidenced by colocalization with CD11b (Fig. 4). Quantitative RT-PCR confirmed the intratumoral induction of mouse Ym1 RNA within Raji xenografts after intracranial tumor implantation in athymic mice.

In parallel, we hypothesized that intratumoral macrophages in human PCNSL would also exhibit features of M2 polarization, induced by IL-4. Given that Ym1 is a mouse-specific macrophage marker and that only a subset of macrophage polarization markers apply from one species to another (23), we focused on the identification of macrophage polarization markers, which are relevant in human lymphoma. Recent studies have suggested that factor XIIIA is an IL-4-induced marker of M2 activation of human macrophages *in vitro* (25,26). Our own studies of the gene expression of tumor-associated $CD14^+$ macrophages, selected from the cerebrospinal fluid from patients with CNS lymphoma, suggested that factor XIIIA is a candidate marker of tumor macrophages in this disease.[6] In the present study, we used immunohistochemistry to examine the expression of factor XIIIA within PCNSL specimens. Both immunoperoxidase and dual-color immunofluorescence strategies with a monoclonal antibody against factor XIIIA revealed its colocalization with $CD68^+$ macrophages in 15 of 20 diagnostic specimens of large cell PCNSL (Fig. 5). As expected, factor $XIIIA^+$ cells did not coexpress glial fibrillary acidic protein (not shown). Factor $XIIIA^+/CD68^+$ cells also did not express S100, suggesting that these macrophages have not undergone dendritic cell maturation. In addition, factor $XIIIA^+$ macrophages were often detected in close proximity to the tumor vasculature (Fig. 5A). By contrast, significant numbers of factor $XIIIA^+$ macrophages were rare in eight consecutive specimens of nodal large B-cell lymphomas as deduced by a parallel immunohistochemical analysis. These data are consistent with the hypothesis that IL-4, produced by lymphoma cells, tumor endothelia, and/or T cells within PCNSL tumors, stimulates macrophage programming toward a M2 phenotype. We believe

this to be the first evidence of macrophages displaying M2 features in large B-cell lymphoma.

Monitoring intracerebral tumor growth and therapeutic response using BLI

To assess the utility of this CNS lymphoma xenograft model for studying intracranial tumor response to therapy, Raji cells were modified with luciferase lentivirus and thereby enabled for *in vivo* BLI. Results in Fig. 6 show a significant correlation between bioluminescence signal and Raji cell number *in vitro* ($R^2 = 0.98$). Analysis of the kinetics of intracranial xenograft growth indicated two phases: a slow growth phase between days 0 and 10 followed by rapid, log-phase growth. Untreated, the median survival of mice bearing intracranial lymphoma in this model was only 13 days.

We next investigated the response of intracranial luciferase-modified Raji xenografts to temozolomide, an alkylating agent now commonly used in PCNSL therapy, both during induction therapies, either as monotherapy or in combination with methotrexate and as means of salvage (27–30). A short course of temozolomide (250 mg/kg/d × 5 days),orally administered, was reproducibly associated with significant delay in tumor progression compared with mock-treated control mice as shown both by BLI and by the delayed onset of neurologic symptoms and prolongation of survival in mice bearing intracerebral lymphoma ($P < 0.0001$; Fig. 6). Whereas Raji cells *in vitro* were found to be sensitive to temozolomide in a dose-dependent manner, *in vivo* Raji tumors rapidly exhibited resistance to this agent, and overall survival of treated mice bearing CNS lymphoma xenografts was not extended beyond 23 days even when the dose of temozolomide was increased to 300 mg/kg/d.

We hypothesized that high constitutive expression of the DNA repair enzyme O^6-methylguanine DNA methyltransferase (MGMT) could account for the relative resistance to temozolomide (11). Given that methylation of the MGMT promoter has been shown to predict favorable response to temozolomide in glioblastoma (31),we tested for this possibility using methylation-specific PCR and were unable to detect DNA methylation of the MGMT promoter in Raji cells. The lack of MGMT promoter methylation was consistent with the results of immunoblot analysis for MGMT protein, which revealed high constitutive expression of MGMT protein by Raji lymphoma cells, compared with four of five glioblastoma xenografts derived from distinct patient tumors (data not shown). These results suggest that lack of MGMT promoter methylation, high constitutive MGMT expression, and possibly other survival signals including the activation of STAT6 signaling may contribute to relatively high alkylator resistance in this CNS lymphoma model.

Discussion

We show that the intracerebral growth of Raji lymphoma cells in athymic mice recapitulates several molecular and histopathologic features of PCNSL pathogenesis, supporting the use of this model for studies of novel agents that selectively address resistance mechanisms identified in this rare variant of non-Hodgkin’s lymphoma. In comparison with prior studies of orthotopic glioma xenografts (11),intracerebral Raji xenografts are moderately sensitive to the alkylating agent temozolomide and exhibit expression of CD20, Bcl-6, MUM-1, IL-4, activated STAT6, Pim-2 kinase, and cathepsin D as well as tumor macrophages displaying

M2 features, reflecting molecular and cellular characteristics defined in PCNSL. We believe this to be the first model of CNS lymphoma to recapitulate multiple molecular and histopathologic features of the disease. Further, we show the first application of bioluminescence to monitor tumor progression and response in a highly infiltrative orthotopic xenograft model of CNS lymphoma.

In this study, we confirm our original observation regarding the expression of IL-4 by B lymphoma cells in CNS lymphoma and directly show its constitutive expression by lymphoma cells in tissue culture and *in vivo*. We propose a model in which IL-4 expression by lymphoma cells has multiple prosurvival functions in these tumors: (*a*) IL-4 expression may potentiate antiapoptotic mechanisms in B lymphoma cells (32,33); this is supported by our prior demonstration that PCNSL tumors with foci of strong STAT6 activation are associated with resistant disease and short survival (7). (*b*) IL-4 may regulate tumor angiogenesis (34–36). (*c*) IL-4 may regulate macrophage differentiation to a M2 phenotype, which promotes tissue remodeling, tumor progression, and tumor-associated immunosuppression (18,26,37).

Macrophages exhibit diverse functional programs in response to environmental signals. Classically activated macrophages, denoted as M1, are characterized by high intrinsic cytotoxic activity against tumor cells by the release of toxic intermediates such as nitric oxide, reactive oxygen intermediates, and tumor necrosis factor. There is increasing evidence that anti-inflammatory molecules such as IL-4, IL-13, IL-10, glucocorticoids, and transforming growth factor-β induce a distinct alternative activation of macrophages, generally denoted as M2. M2 macrophages are involved in Th2 responses and promote wound healing, angiogenesis, and tumor progression. The generation of M2 macrophages attenuates adaptive immunity by down-modulating M1 differentiation and the inhibition of $CD4^+$ T-cell-mediated immune reactions (38,39). The production of CCL17 and IL-10 by M2 macrophages has been shown to negatively regulate the generation of M1 macrophages (39).

Using a mouse model of multiple sclerosis, experimental autoimmune encephalomyelitis (EAE), several investigators have shown an inverse relationship between IL-4 expression in the CNS and the severity of EAE clinical disease (40– 42). Autoimmune T cells mediate demyelination and inflammation in this model. Several lines of evidence suggest that IL-4 reduces the severity of EAE through the induction of M2 features of brain microglia (myeloid lineage cells resident in the CNS). Macrophages classically activated by IFN-γ (M1 macrophages) produce nitric oxide, are proinflammatory, and drive chronic inflammation and tissue injury in EAE (40). The classic activation of macrophages to a M1 phenotype is inhibited by M2 macrophages. As above, M2 macrophages in mice are distinguished by expression of the chitinase family protein Ym1, a mouse-specific, IL-4 target gene, induced by at least 70-fold in multiple macrophage populations and an accepted marker of murine M2 macrophages (23,24). Mice genetically deficient in IL-4 expression exhibited significantly more severe EAE, with absent Ym1-expressing microglia and increased numbers of lymphocytes and peripheral infiltrating macrophages (40). Thus, IL-4 production within the CNS has been shown previously to induce M2 macrophages, which attenuate inflammation in EAE. These results have important implications regarding the

mechanisms by which an immunosuppressive microenvironment is maintained within the brain under normal conditions and the potential pathophysiologic mechanisms that may be subverted by IL-4-producing tumors such as PCNSL to suppress the immune response.

It is particularly noteworthy that Raji cell growth within the brains of athymic mice is highly aggressive in the absence of additional, exogenous immunosuppression. To prevent xenograft rejection, Clynes et al. used total body irradiation (3.0 cGy) to facilitate the tumorigenesis of 5×10^6 Raji cells subcutaneously implanted in athymic mice (43). By contrast, we determined that the intracerebral growth of a smaller inoculum of Raji cells (5×10^5 cells) produced tumors in 100% of athymic mice without immune suppression induced by chemotherapy or irradiation before tumor implantation ($n = 50$ mice). The parallel, subcutaneous, flank implantation of the same inoculum of Raji lymphoma cells failed to elicit tumor growth in three of three immunosuppressed mice.

We hypothesize that, based on its capacity to promote B-cell survival, to stimulate angiogenesis and to suppress the immune response through the M2 polarization of tumor macrophages, intratumoral IL-4 expression may significantly contribute to CNS lymphomagenesis. For these reasons, we suggest that pharmacologic antagonists of IL-4 signaling may facilitate apoptotic response in the treatment of CNS and systemic B-cell malignancies as well.

The evidence for M2 differentiation of a subset of intratumoral macrophages in CNS lymphoma, as shown by their expression of the IL-4 target genes, Ym1 or factor XIIIA, has implications regarding the clinical evaluation of macrophage content in pathologic specimens as a predictor of prognosis in non-Hodgkin’s lymphoma (44–46). Because CD68 is expressed by multiple subpopulations of tumor-associated macrophages in humans, including M1 and M2 phenotypes, the utility of this antigen as a prognostic marker may be limited given that it reflects the total macrophage population, including subtypes that are divergently polarized with different functional properties. Clearly, additional studies are needed to identify phenotypic markers that delineate M1-type versus M2-type macrophage polarization in human cancer. Further studies are needed to evaluate the significance of these macrophage phenotypes as well. The determination of the relative proportion of intratumoral subpopulations of M1 versus M2 macrophages will likely provide more accurate insight into their prognostic significance than are current approaches based on the immunohistochemical detection of CD68 expression alone.

Acknowledgments

Grant support: NIH Brain Tumor SPORE grant P50 CA097267, National Cancer Institute research career award, G&P Foundation, and American Cancer Society.

We thank Rui Galvao and Dora Ayala Payne for technical assistance and Dr. Ernest H. Rosenbaum for continued support.

References

1. Rubenstein JL, Treseler P, O’Brien JM. Pathology and genetics of primary central nervous system and intraocular lymphoma. Hematol Oncol Clin North Am. 2005; 19:705–717. vii. [PubMed: 16083831]

2. Kadoch C, Treseler P, Rubenstein JL. Molecular pathogenesis of primary central nervous system lymphoma. Neurosurg Focus. 2006; 21:E1. [PubMed: 17134111]
3. Montesinos-Rongen M, Van Roost D, Schaller C, Wiestler OD, Deckert M. Primary diffuse large B-cell lymphomas of the central nervous system are targeted by aberrant somatic hypermutation. Blood. 2004; 103:1869–1875. [PubMed: 14592832]
4. Braaten KM, Betensky RA, de Leval L, et al. BCL-6 expression predicts improved survival in patients with primary central nervous system lymphoma. Clin Cancer Res. 2003; 9:1063–1069. [PubMed: 12631608]
5. Camilleri-Broet S, Criniere E, Broet P, et al. A uniform activated B-cell-like immunophenotype might explain the poor prognosis of primary central nervous system lymphomas: analysis of 83cases. Blood. 2006; 107:190–196. [PubMed: 16150948]
6. Tun HW, Personett D, Baskerville KA, et al. Pathway analysis of primary central nervous system lymphoma. Blood. 2008; 111:3200–3210. [PubMed: 18184868]
7. Rubenstein JL, Fridlyand J, Shen A, et al. Gene expression and angiotropism in primary CNS lymphoma. Blood. 2006; 107:3716–3723. [PubMed: 16418334]
8. Gavrilovic IT, Hormigo A, Yahalom J, DeAngelis LM, Abrey LE. Long-term follow-up of high-dose methotrexate-based therapy with and without whole brain irradiation for newly diagnosed primary CNS lymphoma. J Clin Oncol. 2006; 24:4570–4574. [PubMed: 17008697]
9. Hochberg FH, Baehring JM, Hochberg EP. Primary CNS lymphoma. Nat Clin Pract. 2007; 3:24–35.
10. Sarkaria JN, Yang L, Grogan PT, et al. Identification of molecular characteristics correlated with glioblastoma sensitivity to EGFR kinase inhibition through use of an intracranial xenograft test panel. Mol Cancer Ther. 2007; 6:1167–1174. [PubMed: 17363510]
11. Dinca EB, Sarkaria JN, Schroeder MA, et al. Bioluminescence monitoring of intracranial glioblastoma xenograft: response to primary and salvage temozolomide therapy. J Neurosurg. 2007; 107:610–616. [PubMed: 17886562]
12. Baytel D, Shalom S, Madgar I, Weissenberg R, Don J. The human Pim-2 proto-oncogene and its testicular expression. Biochim Biophys Acta. 1998; 1442:274–285. [PubMed: 9804974]
13. Rubenstein JL, Fridlyand J, Abrey L, et al. Phase I study of intraventricular administration of rituximab in patients with recurrent CNS and intraocular lymphoma. J Clin Oncol. 2007; 25:1350–1356. [PubMed: 17312328]
14. Wright G, Tan B, Rosenwald A, Hurt EH, Wiestner A, Staudt LM. A gene expression-based method to diagnose clinically distinct subgroups of diffuse large B cell lymphoma. Proc Natl Acad Sci U S A. 2003; 100:9991–9996. [PubMed: 12900505]
15. Dai H, Li R, Wheeler T, et al. Pim-2 upregulation: biological implications associated with disease progression and perinueral invasion in prostate cancer. Prostate. 2005; 65:276–286. [PubMed: 16015593]
16. Ayala GE, Dai H, Ittmann M, et al. Growth and survival mechanisms associated with perineural invasion in prostate cancer. Cancer Res. 2004; 64:6082–6090. [PubMed: 15342391]
17. Roy S, Josephson SA, Fridlyand J, et al. Protein biomarker identification in the CSF of patients with CNS lymphoma. J Clin Oncol. 2008; 26:96–105. [PubMed: 18056677]
18. Gordon S. Alternative activation of macrophages. Nat Rev Immunol. 2003; 3:23–35. [PubMed: 12511873]
19. Van Ginderachter JA, Movahedi K, Hassanzadeh Ghassabeh G, et al. Classical and alternative activation of mononuclear phagocytes: picking the best of both worlds for tumor promotion. Immunobiology. 2006; 211:487–501. [PubMed: 16920488]
20. Gordon S, Taylor PR. Monocyte and macrophage heterogeneity. Nat Rev Immunol. 2005; 5:953–964. [PubMed: 16322748]
21. Luo Y, Zhou H, Krueger J, et al. Targeting tumor-associated macrophages as a novel strategy against breast cancer. J Clin Invest. 2006; 116:2132–2141. [PubMed: 16862213]
22. Mantovani A, Sozzani S, Locati M, Allavena P, Sica A. Macrophage polarization: tumor-associated macrophages as a paradigm for polarized M2 mononuclear phagocytes. Trends Immunol. 2002; 23:549–555. [PubMed: 12401408]

23. Raes G, Van den Bergh R, De Baetselier P, et al. Arginase-1and Ym1are markers for murine, but not human, alternatively activated myeloid cells. J Immunol. 2005; 174:6561. author reply 6562. [PubMed: 15905489]
24. Welch JS, Escoubet-Lozach L, Sykes DB, Liddiard K, Greaves DR, Glass CK. TH2 cytokines and allergic challenge induce Ym1 expression in macrophages by a STAT6-dependent mechanism. J Biol Chem. 2002; 277:42821–42829. [PubMed: 12215441]
25. Torocsik D, Bardos H, Nagy L, Adany R. Identification of factor XIII-A as a marker of alternative macrophage activation. Cell Mol Life Sci. 2005; 62:2132–2139. [PubMed: 16132226]
26. Martinez FO, Gordon S, Locati M, Mantovani A. Transcriptional profiling of the human monocyte-to-macrophage differentiation and polarization: new molecules and patterns of gene expression. J Immunol. 2006; 177:7303–7311. [PubMed: 17082649]
27. Issa S, Hwang J, Karch J, et al. Treatment of primary CNS lymphoma with induction high-dose methotrexate, temozolomide, rituximab followed by consolidation cytarabine/etoposide : a pilot study with biomarker analysis. Proc Am Soc Hematol. 2007; 110:1364.
28. Herrlinger U, Kuker W, Platten M, Dichgans J, Weller M. First-line therapy with temozolomide induces regression of primary CNS lymphoma. Neurology. 2002; 58:1573–1574. [PubMed: 12034807]
29. Reni M, Mason W, Zaja F, et al. Salvage chemotherapy with temozolomide in primary CNS lymphomas: preliminary results of a phase II trial. Eur J Cancer. 2004; 40:1682–1688. [PubMed: 15251157]
30. Wong ET. Salvage therapy for primary CNS lymphoma with a combination of rituximab and temozolomide. Neurology. 2005; 64:934. author reply. [PubMed: 15753455]
31. Hegi ME, Diserens AC, Gorlia T, et al. MGMT gene silencing and benefit from temozolomide in glioblastoma. N Engl J Med. 2005; 352:997–1003. [PubMed: 15758010]
32. Dancescu M, Rubio-Trujillo M, Biron G, Bron D, Delespesse G, Sarfati M. Interleukin 4 protects chronic lymphocytic leukemic B cells from death by apoptosis and upregulates Bcl-2 expression. J Exp Med. 1992; 176:1319–1326. [PubMed: 1402678]
33. Conticello C, Pedini F, Zeuner A, et al. IL-4 protects tumor cells from anti-CD95 and chemotherapeutic agents via up-regulation of antiapoptotic proteins. J Immunol. 2004; 172:5467–5477. [PubMed: 15100288]
34. Volpert OV, Fong T, Koch AE, et al. Inhibition of angiogenesis by interleukin 4. J Exp Med. 1998; 188:1039–1046. [PubMed: 9743522]
35. Fukushi J, Ono M, Morikawa W, wamoto Y, Kuwano M. The activity of soluble VCAM-1 in angiogenesis stimulated by IL-4 and IL-13. J Immunol. 2000; 165:2818–2823. [PubMed: 10946314]
36. Fukushi J, Morisaki T, Shono T, et al. Novel biological functions of interleukin-4: formation of tube-like structures by vascular endothelial cells *in vitro* and angiogenesis *in vivo*. Biochem Biophys Res Commun. 1998; 250:444–448. [PubMed: 9753649]
37. Martinez FO, Sica A, Mantovani A, Locati M. Macrophage activation and polarization. Front Biosci. 2008; 13:453–461. [PubMed: 17981560]
38. Schebesch C, Kodelja V, Muller C, et al. Alternatively activated macrophages actively inhibit proliferation of peripheral blood lymphocytes and $CD4^+$ T cells *in vitro*. Immunology. 1997; 92:478–486. [PubMed: 9497489]
39. Katakura T, Miyazaki M, Kobayashi M, Herndon DN, Suzuki F. CCL17 and IL-10 as effectors that enable alternatively activated macrophages to inhibit the generation of classically activated macrophages. J Immunol. 2004; 172:1407–1413. [PubMed: 14734716]
40. Ponomarev ED, Maresz K, Tan Y, Dittel BN. CNS-derived interleukin-4 is essential for the regulation of autoimmune inflammation and induces a state of alternative activation in microglial cells. J Neurosci. 2007; 27:10714–10721. [PubMed: 17913905]
41. Falcone M, Rajan AJ, Bloom BR, Brosnan CF. A critical role for IL-4 in regulating disease severity in experimental allergic encephalomyelitis as demonstrated in IL-4-deficient C57BL/6 mice and BALB/c mice. J Immunol. 1998; 160:4822–4830. [PubMed: 9590229]

42. Falcone M, Bloom BR. A T helper cell 2 (Th2) immune response against non-self antigens modifies the cytokine profile of autoimmune T cells and protects against experimental allergic encephalomyelitis. J Exp Med. 1997; 185:901–907. [PubMed: 9120396]

43. Clynes RA, Towers TL, Presta LG, Ravetch JV. Inhibitory Fc receptors modulate *in vivo* cytoxicity against tumor targets. Nat Med. 2000; 6:443–446. [PubMed: 10742152]

44. Farinha P, Masoudi H, Skinnider BF, et al. Analysis of multiple biomarkers shows that lymphoma-associated macrophage (LAM) content is an independent predictor of survival in follicular lymphoma (FL). Blood. 2005; 106:2169–2174. [PubMed: 15933054]

45. Taskinen M, Karjalainen-Lindsberg ML, Nyman H, Eerola LM, Leppa S. A high tumor-associated macrophage content predicts favorable outcome in follicular lymphoma patients treated with rituximab and cyclophosphamide-doxorubicin-vincristine-prednisone. Clin Cancer Res. 2007; 13:5784–5789. [PubMed: 17908969]

46. Canioni D, Salles G, Mounier N, et al. High numbers of tumor-associated macrophages have an adverse prognostic value that can be circumvented by rituximab in patients with follicular lymphoma enrolled onto the GELA-GOELAMS FL-2000 trial. J Clin Oncol. 2008; 26:440–446. [PubMed: 18086798]

Translational Relevance

Primary central nervous system (CNS) lymphoma is a rare variant of non-Hodgkin's lymphoma and is associated with a distinctly poor prognosis. Here, we report the first intracerebral model of CNS lymphoma, which recapitulates several defined aspects of its molecular pathogenesis. These include the relevant immunophenotype of B-cell differentiation as well as the expression of interleukin-4 (IL-4) by malignant B cells in lymphoma xenografts. IL-4is known to potentiate B-cell survival and to mediate the polarization of tumor macrophages to a M2 or alternative activation state associated with enhanced tumorigenesis. We provide the first evidence for expression of macrophages with M2 features in non-Hodgkin's lymphoma both in the model and in diagnostic specimens of CNS lymphoma. These results have implications regarding the potential effect of therapies, which target the IL-4 pathway, as well as the prognostic significance of macrophage subpopulations within non-Hodgkin's lymphoma.

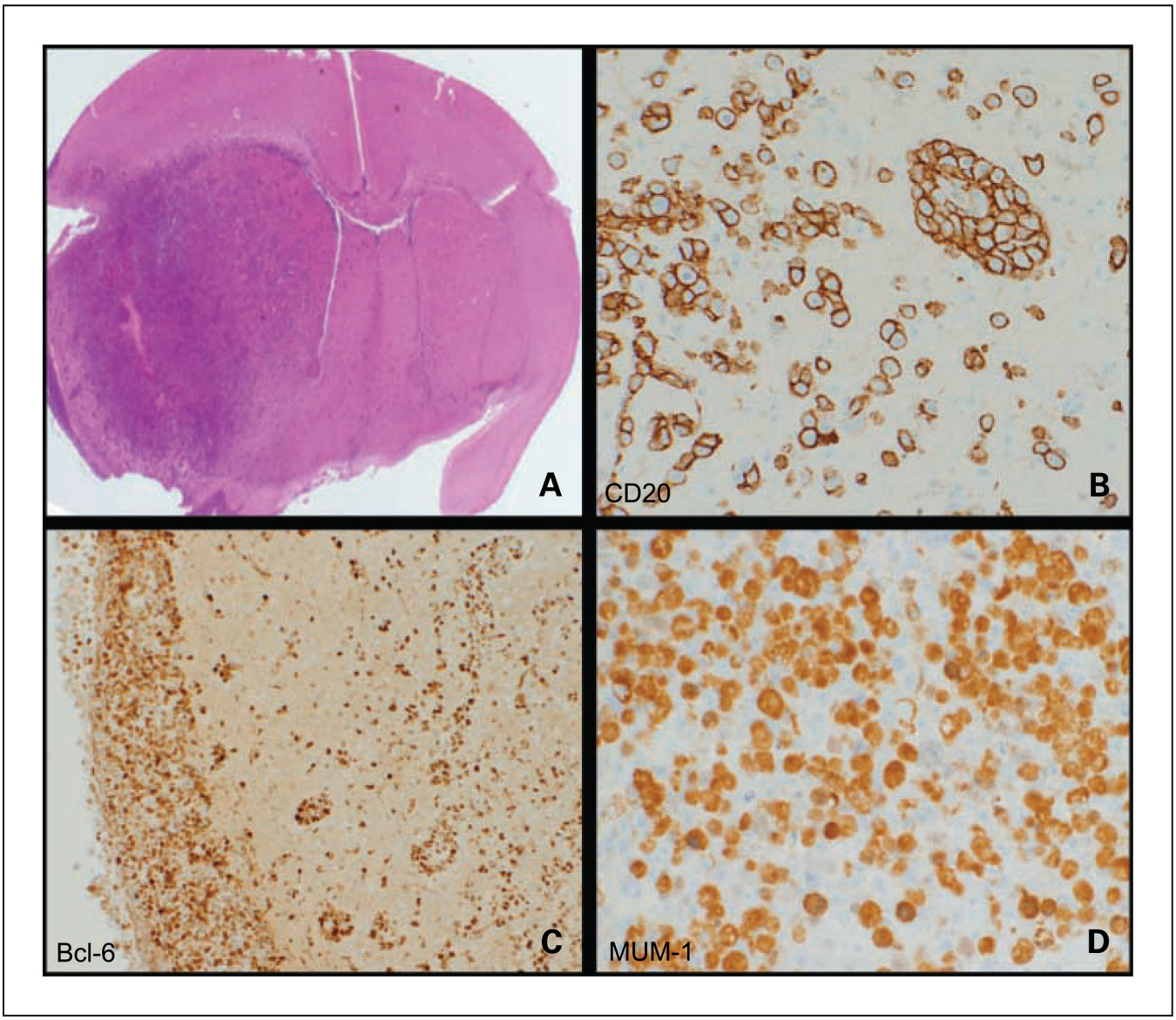

Fig. 1.

Histopathologic analysis of intracerebral model of lymphomatous growth: infiltration and immunophenotype. *A*, intracerebral Raji lymphoma growth in brain is diffusely infiltrative into cerebral cortex, midbrain, contralateral hemisphere, and leptomeninges (H&E) and tumors exhibit the characteristic PCNSL immunophenotype. *B*, $CD20^+$ membrane staining of lymphoma cells with perivascular pattern of infiltration (angiotropism; ×200). *C*, $Bcl\text{-}6^+$ nuclear staining of lymphoma cells that exhibit intense meningeal spread (*left*; ×100). *D*, $MUM\text{-}1^+$ expression by lymphoma cells (×400).

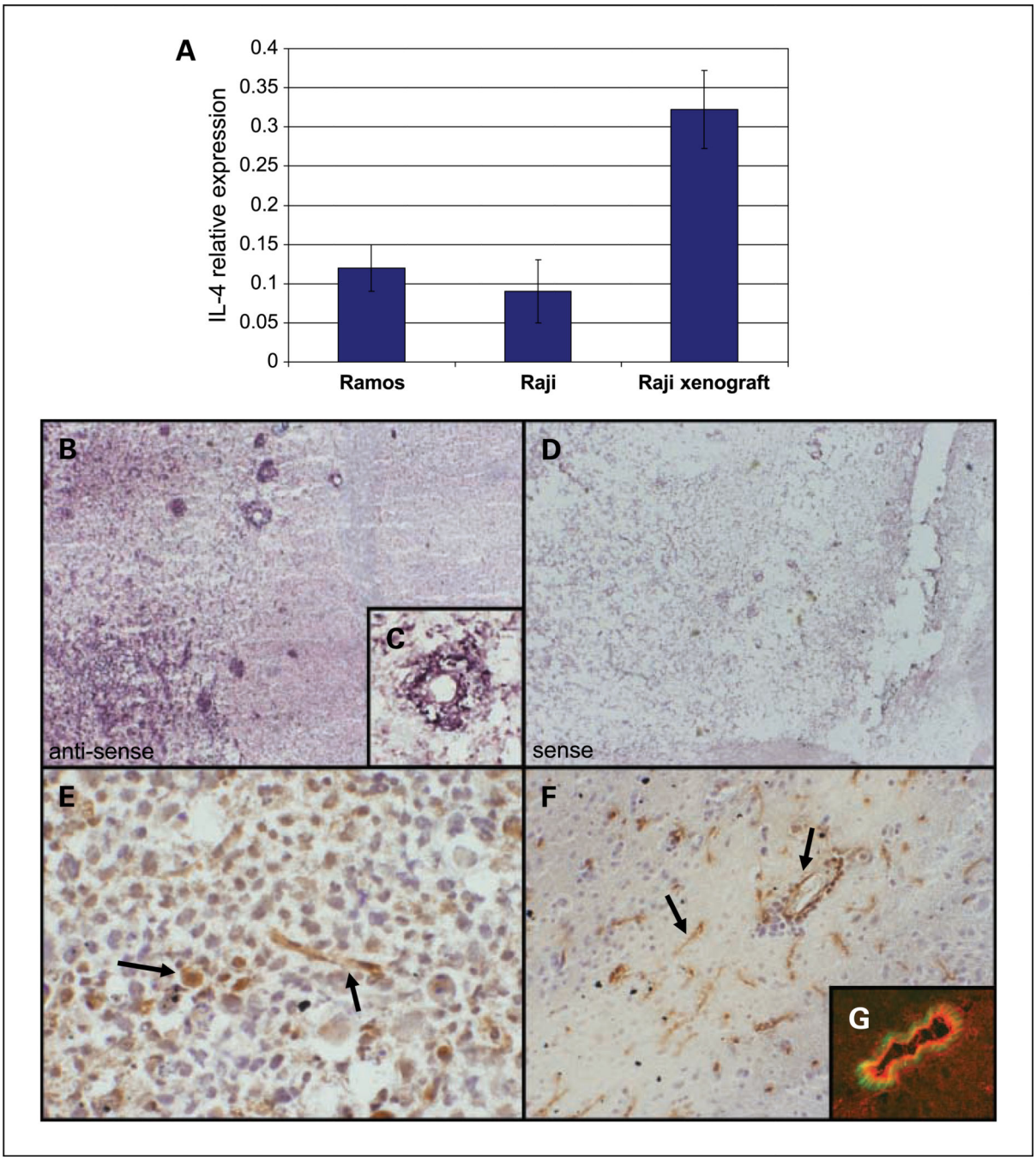

Fig. 2.

IL-4 expression by lymphoma cells in culture and CNS lymphoma xenograft. *A*, quantitative RT-PCR using human-specific IL-4 primers shows constitutive IL-4 expression by Raji and Ramos lymphoma cell lines in culture (normalized to GUS expression). Intracranial implantation of Raji lymphoma cells resulted in a >3-fold increase in relative IL-4 expression ($P < 0.03$). To confirm the species specificity of the primers used, we showed that human IL-4 RNA could not be detected by quantitative RT-PCR using RNA derived from spleen or brain of mice not implanted with intracranial lymphoma cells (data not

shown). *B, in situ* hybridization with an antisense riboprobe against IL-4 shows intratumoral expression in a xenograft model of CNS lymphoma both by tumor cells and by vascular endothelia (×200). There was no evidence for IL-4 expression in normal mouse brain. *C*, higher magnification of a tumor vessel (×400). *D*, a sense riboprobe against IL-4 resulted in no significant hybridization in a parallel section from the same tumor (×200). *E*, expression of IL-4 by tumor macrophage (*large arrow*) and blood vessel (*small arrow*; ×200). *F*, IL-4 expression by microvessels in the periphery of the lymphoma (×100). *G*, dual-color immunofluorescence shows colocalization of IL-4 (*red*) and VWF (*green*) in parallel section of experimental CNS lymphoma model (×400).

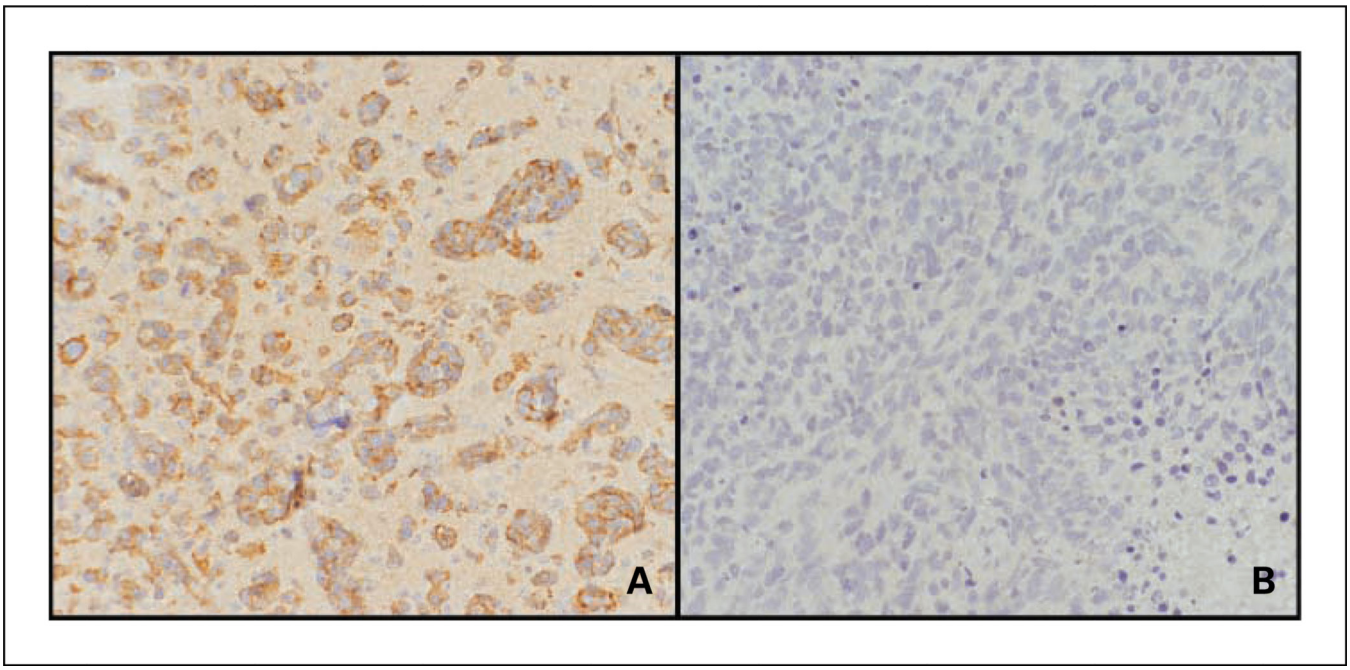

Fig. 3.

Activated STAT6 expression in intracranial lymphoma xenografts. *A*, immunohistochemical detection of activated STAT6 (pSTAT6) in CNS lymphoma model. Lymphoma cells exhibit positive immunoreactivity (×200). *B*, by contrast, glioblastoma xenografts did not express activated STAT6 (×200).

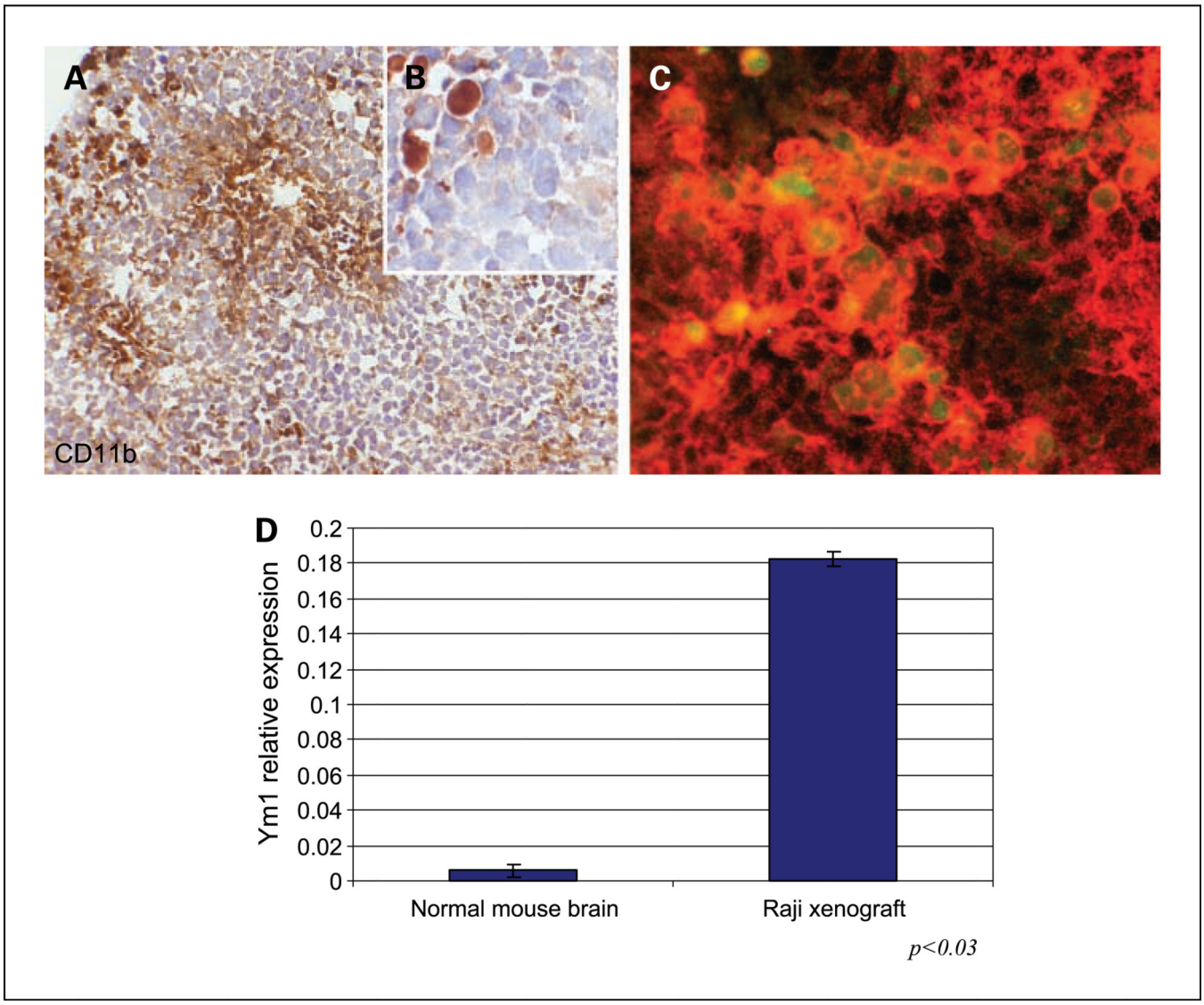

Fig. 4.

Evidence of macrophage recruitment and M2 polarization in intracerebral Raji xenograft model. *A*, micrograph of CD11b immunostaining shows abundant foci of macrophage infiltration within highly cellular CNS lymphoma xenograft (hematoxylin counterstain, ×200). *B*, higher magnification shows specificity of CD11b immunoreactivity by tumor macrophages with absent staining by lymphoma cells (×1,000). *C*, fluorescently labeled antibodies were used to show the presence of intratumoral macrophages using CD11b (Alexa Fluor 594). M2 macrophages were positive for CD11b and Ym1 (Alexa Fluor 488). The merged image indicates M2 macrophages exhibiting cytoplasmic expression of Ym1 by $CD11b^+$ macrophages. *D*, quantitative RT-PCR was used to confirm increased RNA levels of mouse Ym1 associated with intracerebral lymphoma growth.

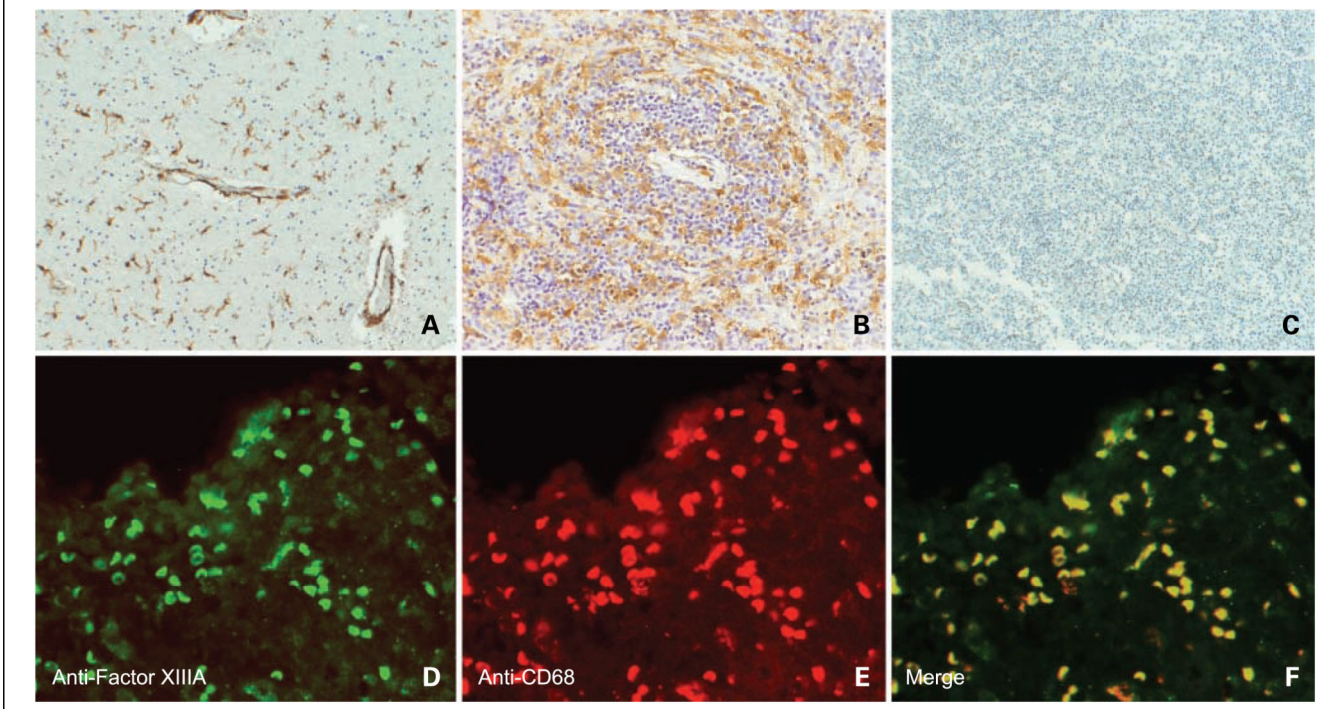

Fig. 5.

Evidence of M2 macrophages within human PCNSL tumors as shown by factor XIIIA expression. Immunohistochemistry reveals factor XIIIA expression by tumor macrophages within two representative diagnostic specimens of PCNSL (*A*, low-density tumor with perivascular macrophages; *B*, high tumor cell density). *C*, absent factor XIIIA expression in a specimen of nodal large B-cell lymphoma (hematoxylin counterstain, ×200). *D*, immunofluorescence image of factor XIIIA expression within a diagnostic specimen of lymphoma. Factor XIIIA^{+} cells were visualized using Alexa Fluor 488. *E*, CD68^{+} macrophages were visualized using Alexa Fluor 594. *F*, merged image shows colocalization of factor XIIIA and CD68. Factor XIIIA did not colocalize with S100 or glial fibrillary acidic protein and was not expressed in specimens of normal brain (data not shown).

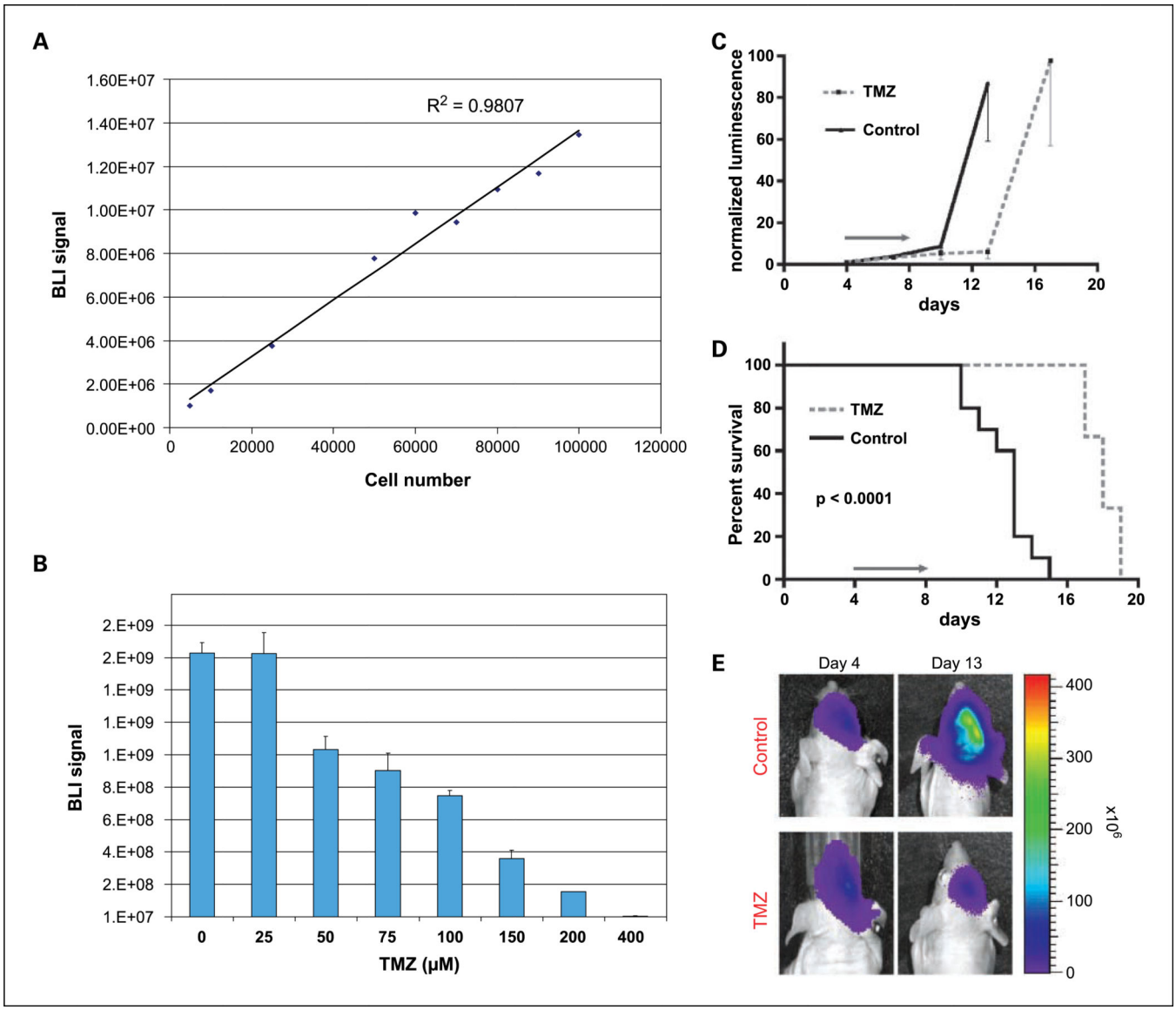

Fig. 6.

Bioluminescence model of CNS lymphoma and *in vivo* assessment of temozolomide response. *A*, correlation between bioluminescence signal and Raji lymphoma cell number *in vitro*. *B*, *in vitro* sensitivity of Raji lymphoma cells to temozolomide. Raji-fl cells were plated as triplicates in six-well plates and treated with the indicated doses of temozolomide or DMSO vehicle alone as control. Cells were treated three times at 24 h intervals. Three days after finishing treatment, cell viability was assessed by quantifying bioluminescence signal, which correlated with the number of metabolically active cells. *C*, normalized luminescence signal for control and temozolomide-treated groups. BLI signal correlates with degree of intracranial tumor burden. The treatment group received five daily doses of temozolomide at 50 mg/kg by oral gavage for a total dose of 250 mg/kg/d. In this experiment, temozolomide was administered between days 4 and 8 after tumor engraftment. The control group received similar volumes of Ora-Plus vehicle according to the same

schedule. *D*, Kaplan-Meier analysis shows survival prolongation associated with short course of temozolomide treatment ($P < 0.0001$, log-rank). *E*, evidence for temozolomide-induced response as shown by BLI.